

# Irisin attenuates inflammation in a mouse model of ulcerative colitis by altering the intestinal microbiota

LU XIN HUANGFU<sup>1,2\*</sup>, XIN TONG CAI<sup>3\*</sup>, JING NAN YANG<sup>4</sup>, HUI CHAO WANG<sup>5</sup>,  
YU XIA LI<sup>4</sup>, ZHI FENG DAI<sup>4</sup>, RUI LIN YANG<sup>4</sup> and XU HONG LIN<sup>4</sup>

<sup>1</sup>Department of Gastroenterology, Huaihe Hospital of Henan University, Kaifeng, Henan 475000; <sup>2</sup>Department of Geriatrics, Henan Provincial People's Hospital; <sup>3</sup>Department of Pathology, The Third Affiliated Hospital of Zhengzhou University, Zhengzhou, Henan 450000; <sup>4</sup>Department of Clinical Laboratory, Translational Medicine Center, Huaihe Hospital of Henan University; <sup>5</sup>Department of Nephrology, The First Affiliated Hospital of Henan University, Kaifeng, Henan 475000, P.R. China

Received July 14, 2019; Accepted May 13, 2020

DOI: 10.3892/etm.2021.10868

**Abstract.** Evidence has demonstrated that the gut microbiota, which consists of probiotics and pathogenic microorganisms, is involved in the initiation of ulcerative colitis (UC) via the dysregulation of intestinal microflora and normal immune interactions, which ultimately leads to intestinal mucosal dysfunction. Irisin is released from muscle cells and displays anti-inflammatory effects; however, the mechanisms underlying irisin-mediated anti-inflammatory effects in UC have not been previously reported. In the present study, mice were divided into the following four groups: i) Control; ii) irisin; iii) dextran sulfate sodium (DSS) salt; and iv) DSS + irisin. Subsequently, the effects of irisin were investigated by observing alterations in intestinal microbes. Irisin significantly reduced the degree of inflammation in UC by reversing alterations to the macroscopic score, histological score, number of CD64<sup>+</sup> cells and inflammatory cytokine alterations ( $P < 0.05$ ). Analysis of the microbial diversity in the stools of mice with active UC indicated that the five bacteria that displayed the greatest alterations in relative abundance were *Alloprevotella*, *Bacteroides*, *Lachnospiraceae-UCG-001*, *Prebotellaceae-UCG-001* and *Rikenellaceae-RCB-gut-group*. Furthermore, *Bacteroides* were positively correlated with the histopathological score ( $P = 0.001$ ;  $R = 0.977$ ) and interleukin (IL)-23 levels ( $P = 0.008$ ;  $R = 0.924$ ). *Alloprevotella* ( $P = 0.001$ ;

$R = -0.943$ ), *Lachnospiraceae-UCG-001* ( $P = 0.000$ ;  $R = -0.973$ ) and *Rikenellaceae-RCB-gut-group* ( $P = 0.001$ ;  $R = -0.971$ ) were negatively correlated with the histopathological score. Furthermore, *Lachnospiraceae-UCG-001* ( $P = 0.01$ ;  $R = -0.873$ ) and *Rikenellaceae-RCB-gut-group* ( $P = 0.049$ ;  $R = -0.814$ ) were negatively correlated with IL-23 levels. In summary, the results of the present study suggested that irisin improved inflammation in a UC mouse model potentially via altering the gut microbiota.

## Introduction

Ulcerative colitis (UC), a chronic non-specific inflammatory bowel disease, typically starts in the rectum and spreads to the proximal colon in a continuous manner, involving the area surrounding the appendix (1,2). UC is characterized by acute pain, vomiting, weight loss, diffuse mucosal inflammation, diarrhoea and bloody stools. The symptoms affect the quality of life of patients due to a high recurrence rate and the lack of effective therapeutic options (3,4). Furthermore, the mechanisms underlying the pathogenesis of UC have not been fully elucidated. A previous study indicated that UC triggers are primarily associated with the immune system, apoptosis, the physical environment, mental psychology, genetic inheritance and infection (5). The human gut contains >100 trillion microorganisms, including commensals and pathogens (6). A previous study demonstrated that dysregulated interactions between the immune system and the intestinal microbiota might lead to colitis (7). Illumina MiSeq sequencing reports have revealed that the diversity of the gut flora in patients with UC is decreased, with significant differences in the abundance of *Bacteroides* and *Lactobacillus*, compared with healthy controls (8,9). The aforementioned studies indicated that alterations in the gut flora are closely related to the pathogenesis of UC.

First identified in 2012, irisin is a myogenic factor (10) and a soluble polypeptide fragment consisting of 112 amino acids (11), which is cleaved from the precursor protein fibronectin type III domain containing 5 (12). A recent report revealed that irisin serves a key role in the occurrence of metabolic, chronic kidney

**Correspondence to:** Dr Xu Hong Lin, Department of Clinical Laboratory, Translational Medicine Center, Huaihe Hospital of Henan University, 115 Ximen Street, Kaifeng, Henan 475000, P.R. China  
E-mail: 10220017@vip.henu.edu.cn

\*Contributed equally

**Key words:** irisin, ulcerative colitis, inflammation, intestinal microbes, Illumina MiSeq sequencing

and autoimmune diseases (13), and that there is a correlation between irisin and the level of inflammation (14). Furthermore, irisin may display anti-inflammatory effects by regulating the expression of receptors and proteins in macrophages, resulting in a reduction in the release of key proinflammatory factors, including tumour necrosis factor- $\alpha$  (TNF- $\alpha$ ), interleukin (IL)-1 $\beta$  and monocyte chemoattractant protein-1 (15). However, the mechanisms underlying the anti-inflammatory properties of irisin are not completely understood. A previous study demonstrated that low concentrations of irisin increase the expression of Toll-like receptor 4 (TLR4) in macrophages, as well as the ability of macrophages to identify potential pathogens, by indirectly promoting anti-inflammatory effects (16). Furthermore, the protein expression levels of TLR4 and myeloid differentiation factor 88 (MyD88), as well as the phosphorylation level of NF- $\kappa$ B, in macrophages were decreased by high irisin concentrations, leading to a reduction in the release of key proinflammatory cytokines and induction of anti-inflammatory effects (16). Another study demonstrated that irisin can control the inflammatory response and reduce pathological progress in the inflammatory response in a concentration-dependent manner in acute lung injury (17). However, to the best of our knowledge, no previous studies have investigated the role of irisin in UC pathogenesis.

A previous study revealed that plasma irisin levels in sedentary mice with UC fed a high-fat diet were decreased compared with those in mice fed a standard diet (18). Furthermore, our preliminary data (data not shown) suggested that irisin may be negatively correlated with IL-12 and IL-23 levels and the abundance of *Enterococci*, but positively correlated with the abundance of *Lactobacilli*. However, the association between irisin and intestinal microbiota in UC is still not completely understood. Therefore, the present study aimed to investigate the therapeutic effect of exogenous irisin, as well as its underlying mechanisms, in an experimental mouse model of UC.

## Materials and methods

**Chemicals and reagents.** Dextran sodium sulphate (DSS) salt (colitis grade; lot no. Q5756) was obtained from MP Biomedicals, LLC. Recombinant irisin (cat. no. 067-29A) was obtained from Phoenix Pharmaceuticals, Inc. The CD64 antibody (cat. no. B166615) was obtained from BioLegend, Inc.

**Establishment of animal models.** Mice were purchased from the Henan Experimental Animal Center [license no. SCXK (Yu) 2015-0004]. A total of 40 C57/BL mice (age, 6 weeks; average weight, 37.767 $\pm$ 4.487 g) were randomly divided into the following four groups (n=10 per group; five males and five females): i) Control; ii) irisin; iii) UC; and iv) UC + irisin. The mice in each group were kept in different cages and administered the corresponding treatments. The control and irisin groups had access to normal autoclaved water. The UC and UC + irisin groups had access to 4% DSS (dissolved in autoclaved water) via drinking water. From day 1, the irisin and the UC + irisin groups received an intraperitoneal injection of irisin (0.0075  $\mu$ g/g; dissolved in PBS) once a day, the UC group and the control group received an intraperitoneal injection of 0.2 ml of PBS, as described by Asadi *et al* (19). During the study, mice were fed a standard rodent diet and were housed

at 25°C with 12-h light/dark cycles and 45% humidity. Each morning, the mice were weighed, and their faeces, faecal characteristics and general states were observed and recorded. On day 10, mice were humanely sacrificed by cervical dislocation as there were signs that the humane endpoints of the study of weight loss and behavioural changes had been reached. The humane endpoints were: i) General appearance: Very rough coat; ii) mental status: Nearly moribund or coma; iii) behaviour: Extremely low in-cage activity level or violent response to external stimuli; iv) clinical signs: Obvious weight change (~80% of initial body weight or a reduction in weight of ~20%) or rare food and water intake. All efforts were made to minimize animal suffering. The animal experiments were approved by the Medical Ethics Committee of Henan University and performed in accordance with the Guidelines of the Institutional Animal Care and Use Committee (20).

**Body weight, spleen weight, macroscopic score and histological score alterations.** Mice were weighed daily and the spleen weight of each mouse was compared at the end of the experiment. The mice were evaluated using macroscopic and histological scoring systems. The histological score was assessed by hematoxylin and eosin staining of colon sections. Colon tissues were fixed in 4% paraformaldehyde overnight at room temperature and embedded in paraffin. The paraffin embedded colon tissues were cut into 5  $\mu$ m thick slices. From each colon sample 5 sections were evaluated and this was repeated in 10 mice per group. The slices were stained at room temperature for 5 min with hematoxylin and 1 min with eosin. Stained sections were observed under a light microscope with a magnification of x200 in four randomly selected fields of view to evaluate inflammatory cell infiltration and mucosal and epithelial destruction. Tissues were histologically scored by two experienced pathologists independently in a blinded manner, from 0 (no change) to 6 (extensive cell infiltration and tissue damage), according to the Siegmund method (Table SII) (21). The sub-scores of inflammatory cell infiltration and epithelial damage were added and divided by two to form a total histological score. Tissues were macroscopically scored from 0.0 (healthy) to 4.0 (maximal activity of colitis), according to the Murano method (Table SI) (22). The sub-scores of weight loss, stool consistency and occult/gross bleeding were added and divided by three, forming a total macroscopic score.

**Immunofluorescence staining of colon tissue.** Colon tissues were fixed in 4% paraformaldehyde at room temperature overnight, paraffin-embedded, sectioned into 5  $\mu$ m slices, and incubated for 2 h at 60°C. The sections were dewaxed with xylene, hydrated with a descending alcohol series and blocked using 5% BSA (cat. no. 9048-46-8; Sigma-Aldrich; Merck KGaA) at room temperature for 1 h. Antigen retrieval was performed by microwaving the sections. Subsequently, the sections were incubated with a PE-labelled CD64 primary antibody (cat. no. 139303, BioLegend, Inc.; 0.2 mg/ml) at room temperature for 1.5 h, followed by nuclear staining with DAPI for 5 min at room temperature. The sections were sealed with glycerol and observed using a fluorescence microscope with a magnification of x200. CD64 expression was quantified using ImageJ software (version 1.51; National Institutes of Health) according to the following formula: Fluorescence integrated density=region of interest area x mean fluorescence intensity.

**ELISA measurement of IL-12 and IL-23 levels in plasma.** Prior to sacrifice on day 10, whole blood (0.5 ml) was collected from the submandibular vein of each mouse. Blood samples were centrifuged at  $1,509.3 \times g$  for 10 min at  $4^{\circ}\text{C}$  to separate the plasma. Subsequently, plasma levels of IL-12 and IL-23 were measured using Hermes Criterion Biotechnology IL-12 mouse ELISA kits and Hermes Criterion Biotechnology IL-23 mouse ELISA kits respectively (cat. nos. I085 and I114; Elixir Canada Medicine Company Ltd.) according to the manufacturer's protocol.

**Fecal DNA extraction.** On day 10, fecal samples were collected from each mouse. Fecal bacterial DNA was extracted using the TIANamp Stool DNA kit (cat. no. DP328-02; Tiangen Biotech Co., Ltd.) according to the manufacturer's instructions.

**Library preparation and sequencing.** MetaVx™ library preparation and Illumina MiSeq sequencing were conducted at Genewiz, Inc. DNA quantity of the fecal bacterial DNA was determined using a Qubit 2.0 fluorometer (Invitrogen; Thermo Fisher Scientific, Inc.) and a library was prepared using the MetaVx™ Library Preparation kit (Genewiz, Inc.). V3 and V4 are two hypervariable regions of the prokaryotic 16S rDNA (23). The V3 and V4 regions were amplified using the same following primers: Forward, 5'-CCTACGGRBGCASCAGKVRVGAA T-3' and reverse, 5'-GGACTACNVGGGTWTCTAATCC-3'. PCR was performed using 30-50 ng template DNA (EasyTaq® DNA Polymerase, cat. no. AP111-01, TransGen Biotech). The first-round PCR products were used as templates for a second round of amplicon enrichment by PCR ( $94^{\circ}\text{C}$  for 3 min, followed by 24 cycles at  $94^{\circ}\text{C}$  for 5 sec,  $57^{\circ}\text{C}$  for 90 sec and  $72^{\circ}\text{C}$  for 10 sec, and a final extension at  $72^{\circ}\text{C}$  for 5 min). In addition, indexed adapters were added to the ends of the 16S rDNA amplicons to generate indexed libraries that were ready for downstream NGS on the MiSeq platform. The quality and concentration of the library were tested using the Agilent 2100 bioanalyzer (Agilent Technologies Inc.) and Qubit 2.0 fluorometer (Invitrogen; Thermo Fisher Scientific, Inc.), respectively. DNA libraries were multiplexed and loaded on an Illumina MiSeq instrument (Illumina, Inc.) according to the manufacturer's instructions. Sequencing was performed using a 2x300 paired-end configuration and the data were analysed using Miseq Control software (version 2.5.0.5; Illumina, Inc.). To process the raw data, all the forward and reverse reads were assembled in pairs, the sequences containing N in the results were filtered and sequences >200 bp in length were retained. Subsequently, the spliced and filtered sequences were compared with Basic Local Alignment Search Tool (BLAST, <https://blast.ncbi.nlm.nih.gov/Blast.cgi>) match lengths (against reference sequences in the database) to remove the chimera sequence (<90% match). In the operational taxonomic unit (OTU) analysis, the 16S reads were clustered using the VSEARCH software (version 1.9.6; <https://github.com/torognes/vsearch>) with a pair-wise identity cutoff of 97%, and the 16S rRNA reference database was Silva 132 (<https://www.arb-silva.de/search/>). Representative sequences of each OTU were analyzed using the Ribosome Database Program classifier (version 2.2, <http://rdp.cme.msu.edu/classifier/classifier.jsp?jsessionid=D5D6C78C6C197C015E237D0FD7A85246.10.0.0.9>). Bayesian algorithm and the composition of each sample at different species classification levels was calculated. According

to the OTU analysis results, the random sampling method was used to calculate the  $\alpha$  diversity index of Shannon and Chao1, and the dilution curve was obtained. Unweighted unifrac analysis was applied to compare whether there were significant differences in microbial communities among samples. The Bray-Curtis distance matrix among samples was used for PCoA (Principal Coordinate Analysis) to indicate  $\beta$  diversity and the P-value was calculated using a non-parametric MANOVA. To compare the hierarchical relationships among groups, the UPGMA (Unweighted Pair Group Method for Arithmetic Mean) clustering tree was constructed by the non-weighted mean method in hierarchical clustering. Anosim analysis was confirmed according to Bray-Curtis. Linear discriminant analysis effect size analysis was performed by LDA (Linear Discriminant Analysis; [huttenhower.sph.harvard.edu/galaxy](http://huttenhower.sph.harvard.edu/galaxy)) to calculate the impact of species richness on the difference effect and to identify the species with a significant difference. Based on the  $\beta$  diversity distance matrix and environmental factor data, the redundancy analysis was determined.

**Statistical analysis.** Statistical analyses were performed using SPSS software (version 19.0; IBM Corp.). Data are presented as the mean  $\pm$  SD. Values were obtained from 10 animals per group. For normally distributed data, comparisons among multiple groups were analysed by one-way ANOVA followed by Tukey's post hoc test. For non-normally distributed data, comparisons among multiple groups were analysed by the Kruskal-Wallis test followed by the Dunn-Bonferroni post hoc test. Correlations between specific bacteria and the histological score or IL-12/23 levels were determined by Pearson correlation analysis.  $P < 0.05$  was considered to indicate a statistically significant difference.

## Results

**Irisin improves the macroscopic and histopathological scores of UC model mice.** In the UC group, body weight was significantly decreased from day 4-7 compared with the control group ( $P < 0.01$ ; Fig. 1A). Furthermore, the macroscopic ( $P < 0.01$ ; Fig. 1C) and histological ( $P < 0.01$ ; Fig. 1D and E) scores were significantly increased in the UC group compared with the control group. Irisin did not significantly alter the colonic tissues in normal mice; however, irisin decreased the macroscopic ( $P < 0.05$ ) and histological ( $P < 0.05$ ) scores in UC model mice. Furthermore, the spleen weight of the UC group was increased compared with the control group, and irisin treatment decreased UC-mediated alterations to the spleen weight; however, the differences were not statistically significant (Fig. 1B).

**Irisin downregulates the number of CD64<sup>+</sup> cells in colonic tissues in UC model mice.** Compared with the control group, the number of CD64<sup>+</sup> cells in colonic tissues in the irisin group was not significantly altered; however, the UC group displayed a significantly increased number of CD64<sup>+</sup> cells compared with the control group ( $P < 0.01$ ; Fig. 2A and B). CD64 fluorescence staining was significantly decreased in the irisin-treated UC model mice compared with untreated UC model mice ( $P < 0.05$ ; Fig. 2A and B).

**Irisin reduces plasma IL-12 and IL-23 levels in UC model mice.** The levels of IL-12 and IL-23 in the plasma of normal

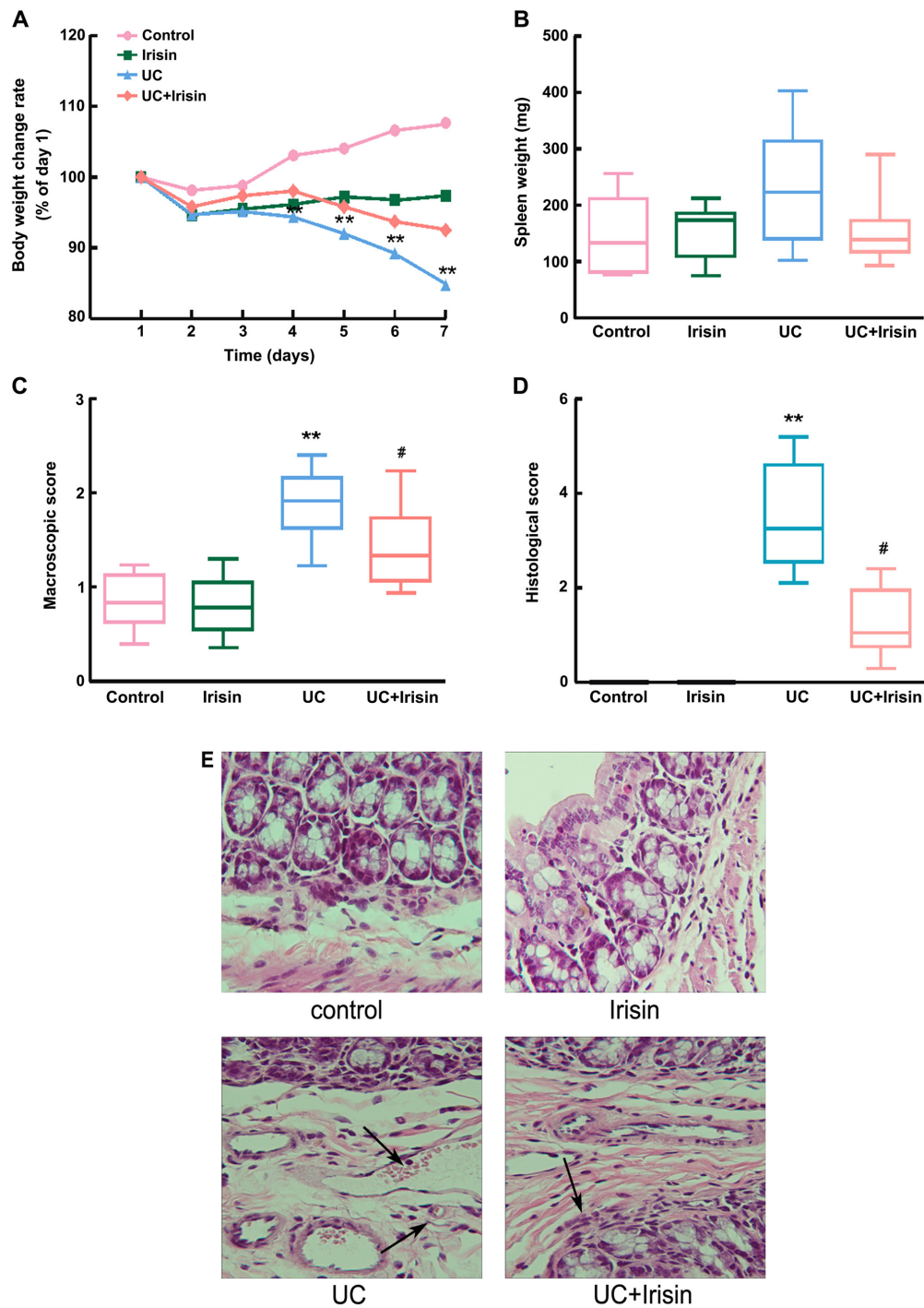


Figure 1. Alterations to body weight, spleen weight, macroscopic score and histological score. (A) Body weight. (B) Spleen weight. (C) Macroscopic score. (D) Histological score. (E) Hematoxylin and eosin staining. x200, black arrows indicate congestion, edema and inflammatory cell infiltration in the colon tissue. \*\*P<0.01 vs. control; #P<0.05 vs. UC. UC, ulcerative colitis.

mice were  $893.15 \pm 222.76$  and  $685.67 \pm 137.55$  pg/ml, respectively. There was no significant difference in IL-12 and IL-23 levels between the control and irisin ( $911.63 \pm 129.57$  and  $698.69 \pm 163.15$  pg/ml, respectively) groups. However, the levels of IL-12 ( $1,147.37 \pm 233.92$ ;  $P < 0.05$ ) and IL-23 ( $1,137.27 \pm 156.49$  pg/ml;  $P < 0.01$ ) in the UC group were significantly increased compared with the control group. Irisin significantly reduced UC-mediated upregulation of IL-12 ( $911.04 \pm 122.78$  pg/ml;  $P < 0.05$ ). In addition, irisin decreased UC-mediated upregulation of IL-23 levels, but the decrease was

not significant (Fig. 3). Collectively, the results suggested that irisin displayed an anti-inflammatory effect in UC model mice.

*Alterations to the gut microbiota structure of UC model mice following treatment with irisin.* A total of 6,064,158 reads and 1,516,039,500 base pairs were analysed in the four groups. Quality filtering on joined sequences was performed, and sequences that did not fulfil the criteria were discarded. Finally, a total of 2,409,318 reads with an average length of 450.78 base pairs were obtained. The multivariate analysis of variance of



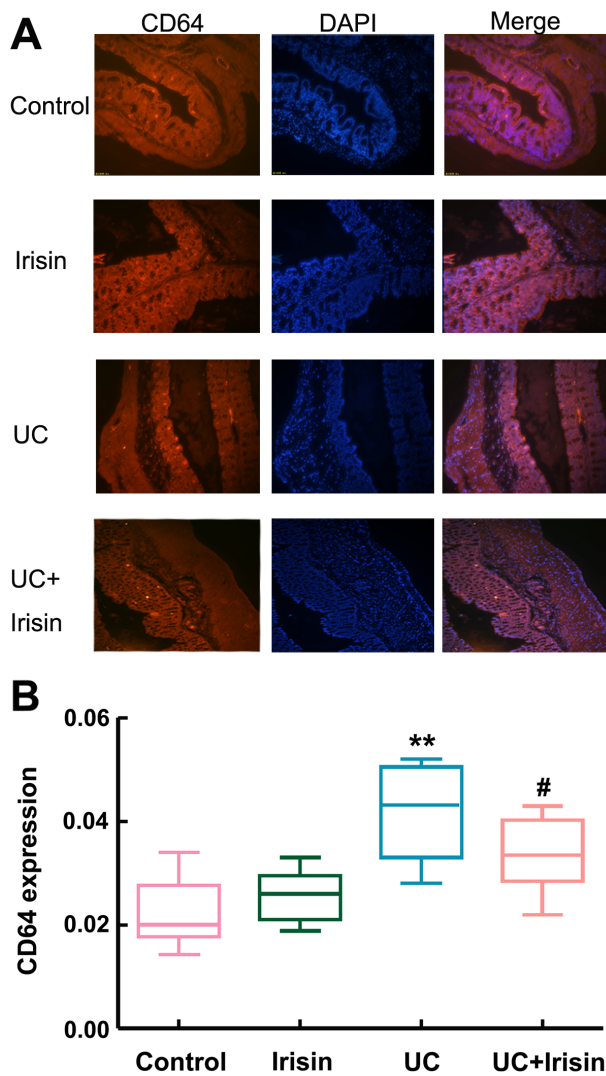


Figure 2. Abundance of CD64<sup>+</sup> cells in the colonic tissues of mice in the four groups. (A) Representative images of CD64 expression in the colonic tissues of the mice x200. (B) Quantification of CD64 expression. \*\*P<0.01 vs. control; #P<0.05 vs. UC. UC, ulcerative colitis.

the PCoA matrix scores indicated that primary coordinate 1 and primary coordinate 2 accounted for 22.94 and 9.84% of the total structural changes, respectively (Fig. 4A). The intestinal flora in control and irisin groups were significantly different from that in UC and UC + irisin groups, which indicated that changes in flora structure play an important role in the pathogenesis of UC. In accordance with UPGMA clustering, the four groups were divided into four different clustering trees (Fig. 4B). The dilution curve analysis indicated that the curves of each group reached a plateau, suggesting that the majority of the microbiota were identified (Fig. 4C). According to the Shannon and Chao1 indices (Fig. 4D and E), the majority of the diversity was identified in all samples. The results indicated that there was a decrease in diversity in UC group compared with control group (P<0.01) for both the Shannon and Chao1 indices. Analysis of the microbial diversity in the stools of mice with active UC indicated that the five bacteria that displayed the greatest alterations in relative abundance were *Alloprevotella*, *Bacteroides*, *Lachnospiraceae-UCG-001*, *Prebotellaceae-UCG-001* and *Rikenellaceae-RCB-gut-group* (Fig. S1).

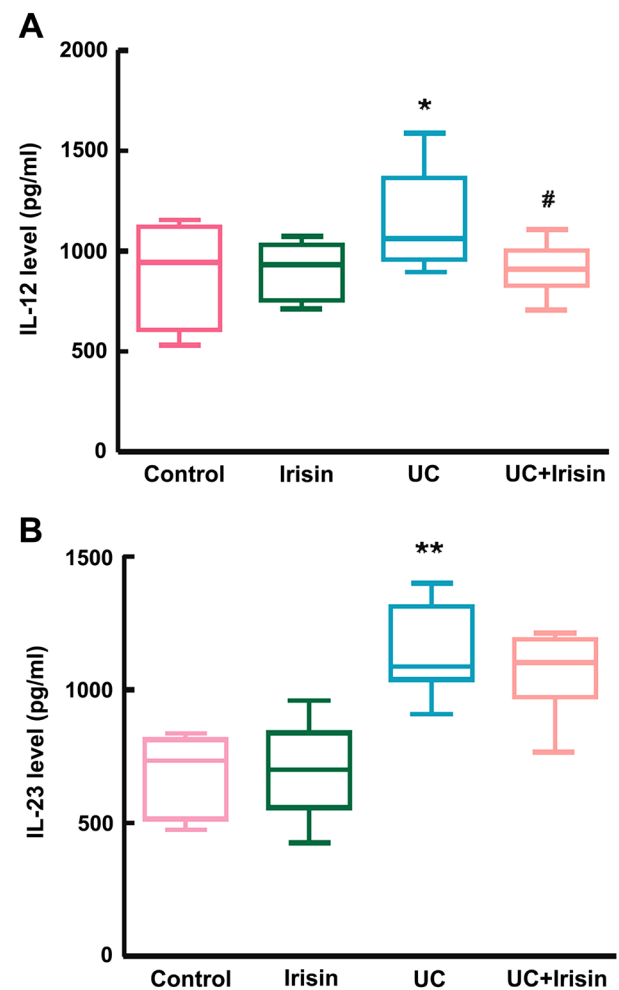


Figure 3. IL-12 and IL-23 levels in the plasma of mice in the four groups. The level of (A) IL-12 and (B) IL-23 in the plasma. \*P<0.05 and \*\*P<0.01 vs. control; #P<0.05 vs. UC. IL, interleukin; UC, ulcerative colitis.

**Irisin alters the gut microbiota composition.** The gut microbiota community structure histograms indicated the microbial species present and their relative abundance (Fig. 5). All samples contained five main phyla: *Bacteroidetes*, *Firmicutes*, *Epsilonbacteraeota*, *Proteobacteria* and *Deferribacteres* (Fig. 5A). The composition of the microbiota in the control and irisin groups was similar. The abundance of *Deferribacteres* in the UC group was lower compared with the control and irisin groups (0.58 vs. 1.03%, 1.10%), and slightly higher in the UC + irisin group (0.89%) compared with the UC group. In addition, the abundance of *Cyanobacteria* (0.52%) and *Patescibacteria* (0.62%) in the UC group was highest among the four groups.

In all samples, 20 main families were identified, including *Lachnospiraceae*, *Bacteroidaceae*, *Muribaculaceae*, *Prevotellaceae*, *Deferribacteres* and *Lactobacillaceae* (Fig. 5B). Following treatment with irisin, the abundance of *Deferribacteres* in the UC model mice was slightly upregulated (from 0.58 to 0.89%); however, the abundance remained lower compared with the control and irisin groups (1.03 and 1.09% respectively). In UC group, the relative abundance of *Lactobacillaceae* (0.99%), *o-Rhodospirillales-Unclassified* (0.67%) and *Staphylococcaceae* (0.89%) were all increased compared with control group. With the treatment of irisin, the abundance of *Lactobacillaceae*

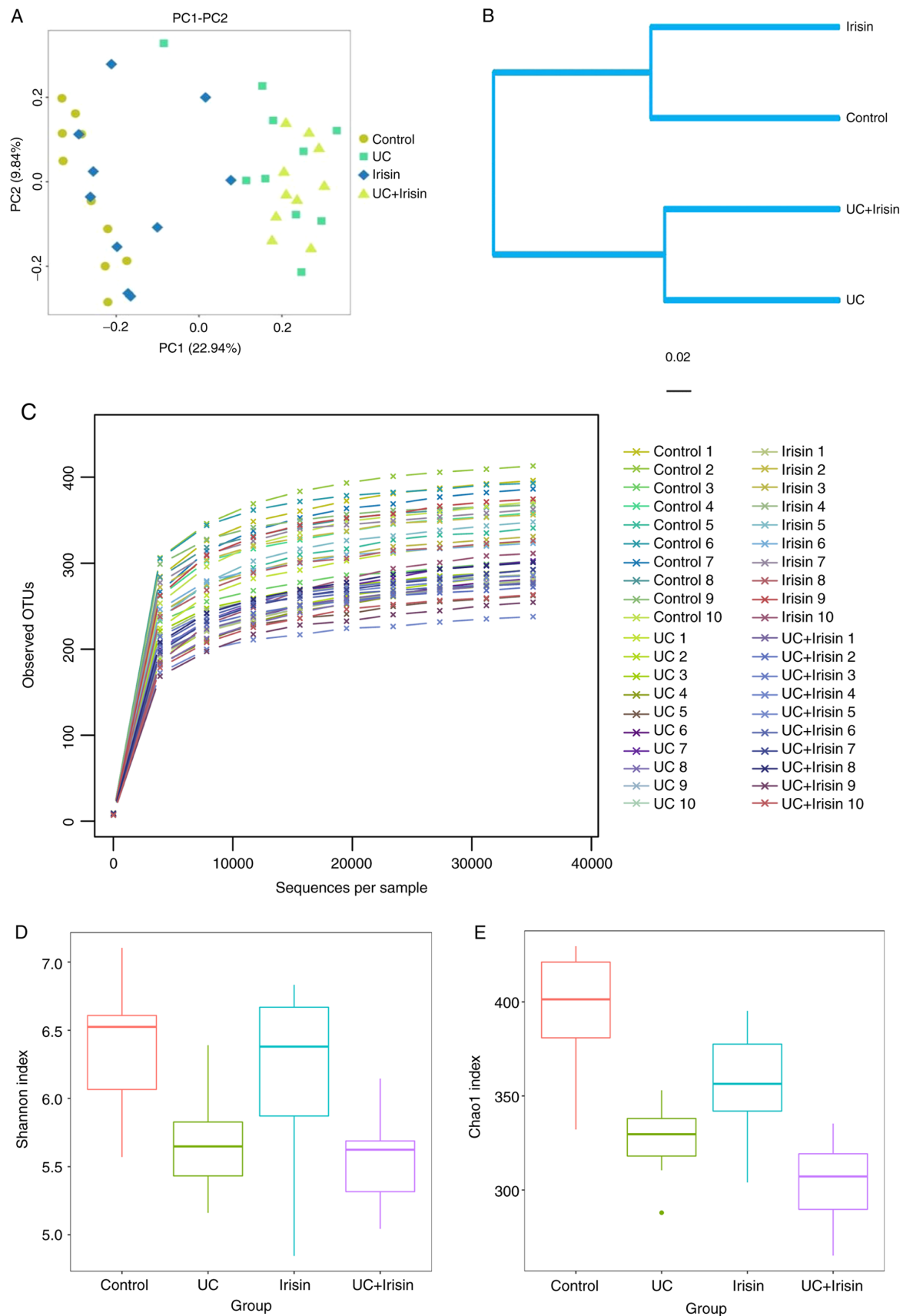


Figure 4. Comparison of  $\beta$  and  $\alpha$  diversity index in the four groups. (A) A principal coordinate analysis was performed using the  $\beta$  diversity metrics of the weighted UniFrac distance in the four groups. There were apparent differences in the composition of the microbial population between the control, UC and UC + irisin groups. (B) Analysis of the unweighted pair group method with arithmetic mean clustering in the four groups. '0.02' represented the scale of the difference between samples. (C) The dilution curve of each sample. (D) Shannon-Wiener, one of the  $\alpha$  diversity indexes, could directly reflect the heterogeneity of a community based on the number of species present and their relative abundance. (E) Chao 1, another  $\alpha$  diversity index, reflects the richness of the community in the sample. The green dot in the UC group represented an outlier. UC, ulcerative colitis; con, control; OUT, operational taxonomic unit; PC, primary coordinate.

(0.66%), *o-Rhodospirillales-Unclassified* (0.31%) and *Staphylococcaceae* (0.40%) were all decreased compared with UC group.

Sequencing data identified 31 genera of microbial flora. The abundance of *Bacteroides*, *Lachnospiraceae-NK4A136-group*, *f-Muribaculaceae-Unclassified*, *Prevotella-1*, *Prevotella-9*, *Prevotellaceae-UCG-001* and *Lachnospiraceae-UCG-001* was changed most (>1% of total composition in all groups). The abundance of *Bacteroides* (8.29 vs. 26.57%) and *Lachnospiraceae-NK4A136-group* (8.38 vs. 11.71%) was higher in the UC group than in the control group. By contrast, the abundance of *f-Muribaculaceae-Unclassified* (11.29 vs. 7.59%), *Prevotella-1* (3.99 vs. 1.00%), *Prevotella-9* (3.88% vs. 0.00%), *Prevotellaceae-UCG-001* (3.55 vs. 0.00%) and *Lachnospiraceae-UCG-001* (1.25 vs. 0.00%) was decreased. Following treatment with irisin, the abundance of *Ruminococcaceae-UCG-014* decreased from 2.05 to 1.25%, which was similar to the control group 0.93%. *Lactobacillus* decreased from 0.99 to 0.66%, which was similar to the control group 0.57% (Fig. 5C).

Furthermore, 31 main species were identified in all four groups. For example, the relative abundance of *g-Bacteroides-Unclassified* was higher in the UC group compared with the control and irisin groups (7.82 vs. 0.38%, 0.90%). However, the relative abundance of *g-Bacteroides-Unclassified* was decreased in the UC + irisin group compared with the UC group (4.62 vs. 7.82%; Fig. 5D).

**Heatmap at different taxonomic levels.** At the phylum level, *Deferribacteres* was present at a lower level in the UC group compared with the other three groups. By contrast, the abundance of *Patescibacteria* and *Cyanobacteria* was higher in the UC group compared with the control group (Fig. 6A). At the class level, the abundance of *Erysipelotrichia* was increased in the UC group compared with the control and irisin groups, and slightly decreased in the UC + irisin group compared with the UC group (Fig. 6B).

**Correlation analysis between alterations to the gut flora and the histopathological score, as well as the plasma levels of IL-12 and IL-23 in the four groups.** A positive association between the histopathological score and IL-12/23 levels was identified (Fig. 7). Compared with the other three groups, the structure of the gut flora in the UC group was more closely related to histopathological score and IL-12/23 levels. In addition, IL-12 served a more important role in the correlation compared with IL-23. Furthermore, the correlation between the top five most variable flora (Fig. S1) in the UC group and IL-12 and IL-23 levels, and histopathological score were analysed (Table SIII). *Bacteroides* was positively correlated with the histopathological score ( $P=0.001$ ;  $R=0.977$ ) and IL-23 levels ( $P=0.008$ ;  $R=0.924$ ). The other three types of microbiota, *Alloprevotella* ( $P=0.001$ ;  $R=-0.943$ ), *Lachnospiraceae-UCG-001* ( $P=0.000$ ;  $R=-0.973$ ) and *Rikenellaceae-RC8-gut-group* ( $P=0.001$ ;  $R=-0.971$ ), were negatively correlated with the histopathological score. *Lachnospiraceae-UCG-001* ( $P=0.01$ ;  $R=-0.873$ ) and *Rikenellaceae-RC8-gut-group* ( $P=0.049$ ;  $R=-0.814$ ) were also negatively correlated with IL-23 levels.

**Analysis of the gut flora structure in the four groups.** The composition of the gut flora was significantly different among the four groups ( $P=0.001$ ;  $R=0.515$ ; Fig. 8). The LDA scores indicated that the *g-Ruminococcaceae-UCG-014* and *g-Family-XIII-UCG-001* played important roles in the UC and irisin groups, respectively (Fig. 9). In the control group, a total of 12 different types of microorganisms (LDA score >3.0) served a vital role in the gut flora structure. In particular, *f-Prevotellaceae* displayed the most significant role (Fig. 9). But the UC + irisin group had no dominant bacteria.

## Discussion

UC is a chronic non-specific inflammatory bowel disease with a high recurrence rate, for which the current therapies are largely ineffective (24). Previous studies have indicated the environment, autoimmunity, psychology and genetic inheritance are closely related to the occurrence of UC (25,26). Therefore, UC is not a disease induced by a single factor. Previous studies have also suggested that the interaction between disordered intestinal flora and an abnormal immune response may lead to intestinal mucosal dysfunction (27). Moreover, dysfunction of the intestinal mucosal barrier may serve as a trigger for UC and is associated with the incidence of disease (28).

Intestinal microorganisms consist of commensal bacteria, probiotics and pathogenic bacteria (29). Under physiological conditions, all types of microorganisms maintain symbiotic or antagonistic relationships in the intestine to form a dynamic and balanced micro-ecological system (30). Healthy intestinal flora can protect the intestine, improve the metabolism, regulate immunity, and help resist inflammation and tumour growth (31,32). Previous studies have reported that exercise optimizes the composition of the intestinal flora and improves intestinal microecology (33,34). Sufficient exercise, for example, 30 min of swimming a day, may amplify the anti-bacterial effect of the intestine and relieve intestinal barrier dysfunction induced by chronic inflammation (35). A previous study revealed that exercise increased the diversity of the intestinal microbiota in professional rugby players and simultaneously reduced the level of inflammatory markers (36). The aforementioned studies indicated that the beneficial effect of exercise is partly due to the increased intestinal microbial diversity that occurs as a result of exercise. Additionally, Allen *et al* (37) revealed that voluntary physical activity alters the intestinal microbes present in mice; however, the mechanisms underlying how movement can alter the flora of the inflammatory intestine are not completely understood.

In the present study, the symptoms of the UC model mice were consistent with the clinical symptoms of patients with UC, and the macroscopic and histological scores of UC model mice were increased compared with the control mice. The relative abundance of *Bacteroides* and *Lachnospiraceae-NK4A136-group* were increased in UC model mice. The levels of inflammatory factors in the plasma decreased in UC model mice following the intraperitoneal injection of irisin, and UC symptoms were also alleviated. Alterations to the relative abundance of *Ruminococcaceae-UCG-014* and *Lactobacillus* in irisin treated mice were identified by sequencing. Furthermore, a previous study reported that the symptoms of DSS-induced UC in mice were improved following HuangQin treatment,

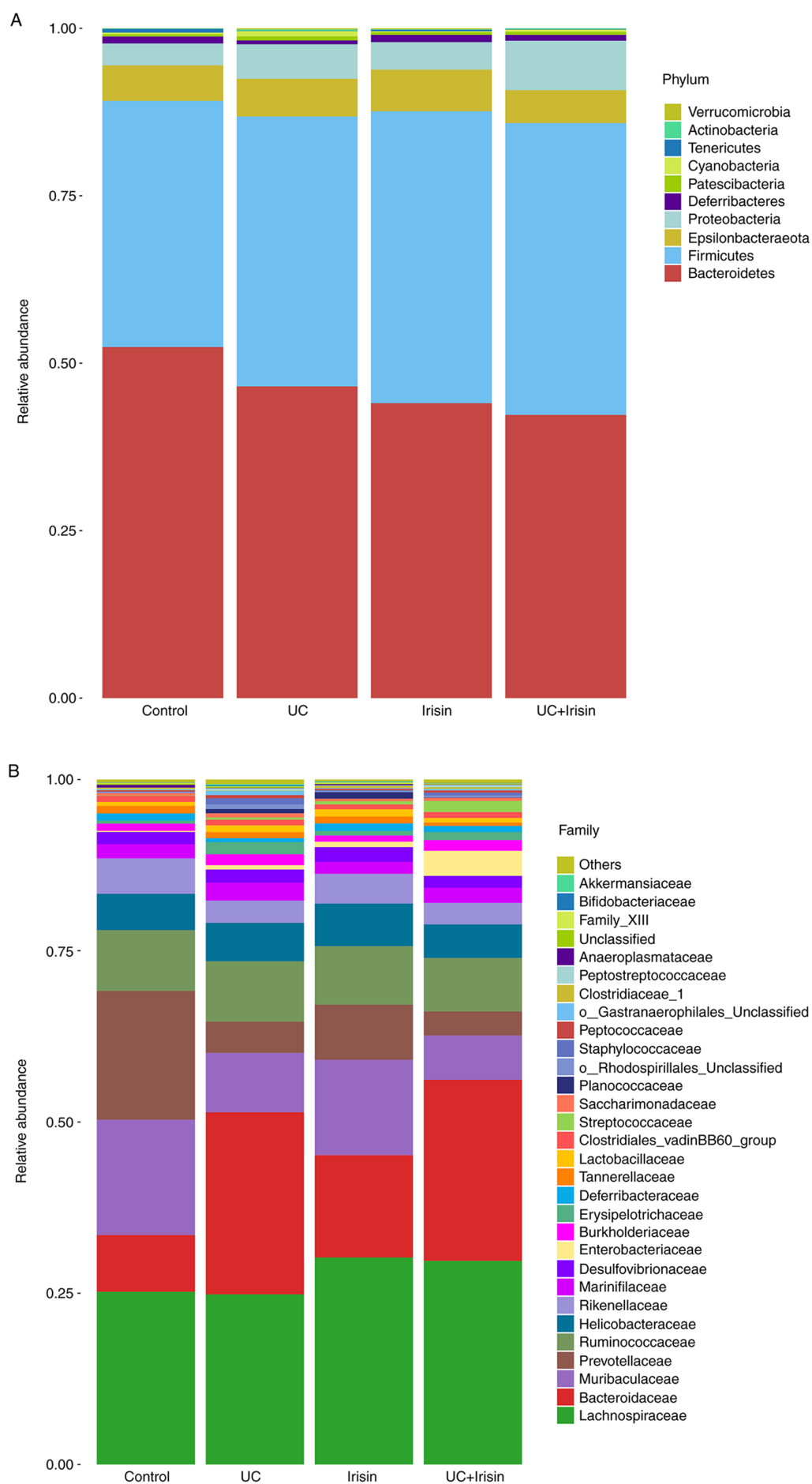


Figure 5. Continued.



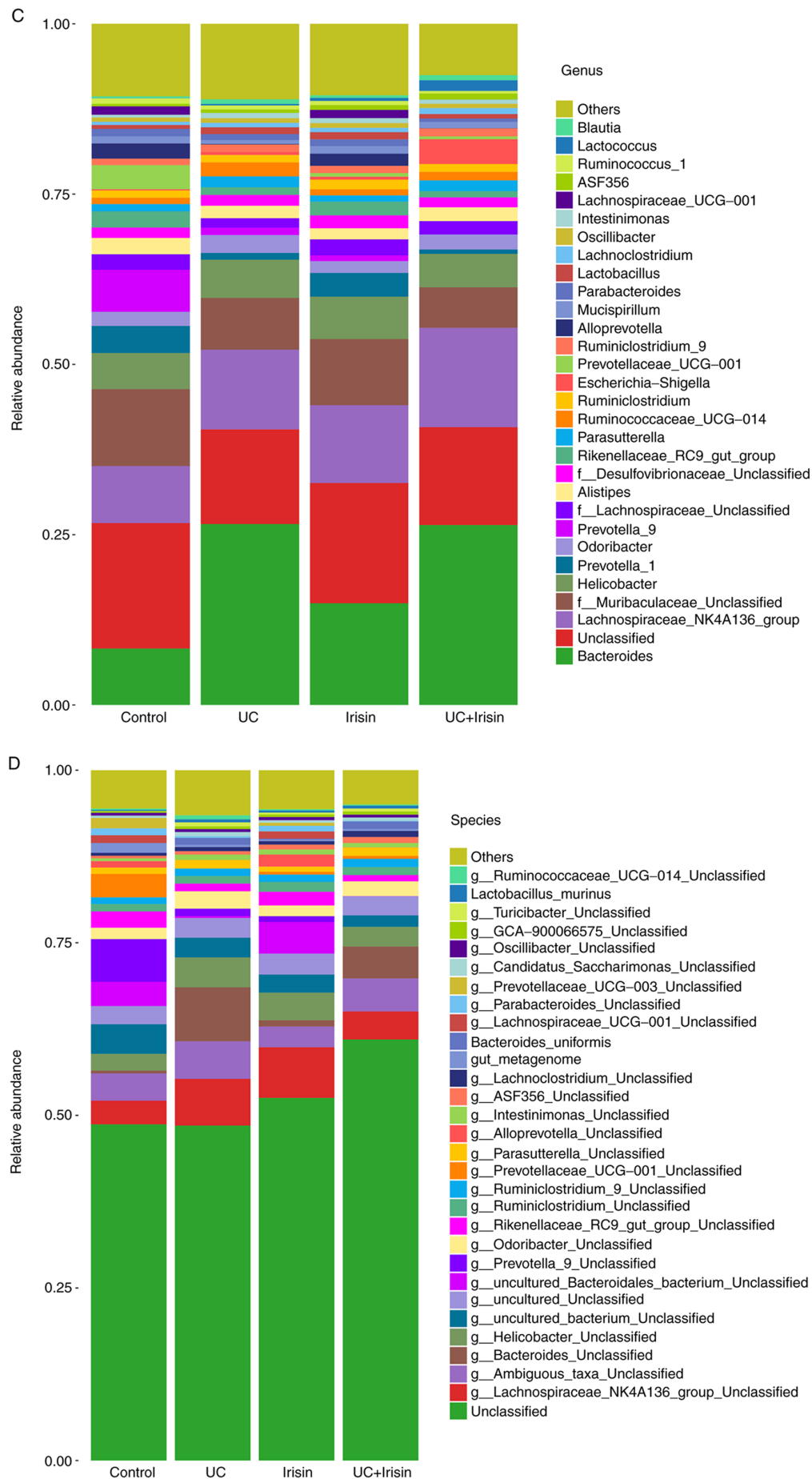


Figure 5. Gut microbial community structure in the four groups. Microbial community structures by (A) phylum, (B) family, (C) genus and (D) species. Con, control; UC, ulcerative colitis.

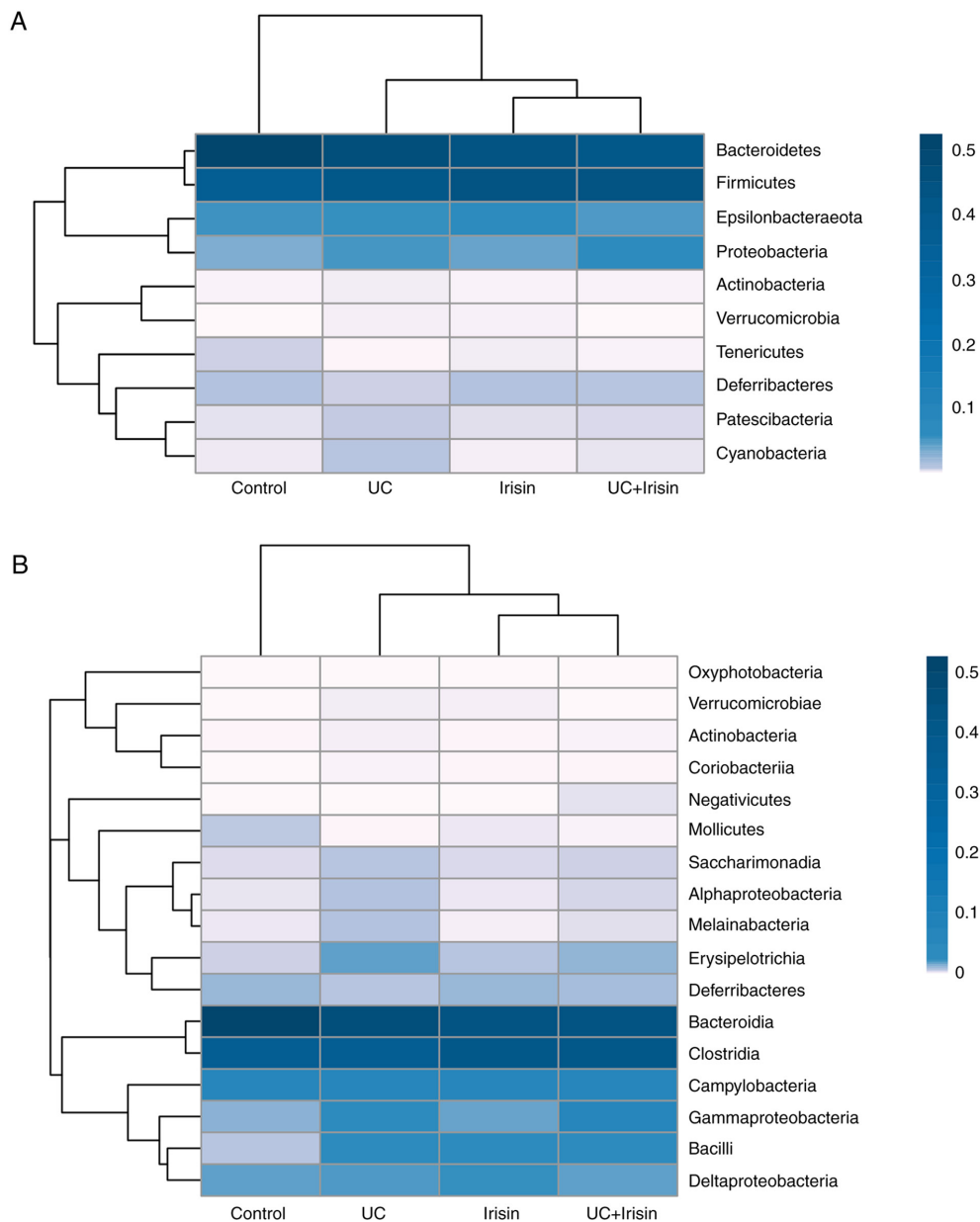


Figure 6. Heatmaps of the gut microbiota in the four groups. A heatmap of the gut microbiota in the four groups at the (A) phylum and (B) class levels. The different shades of blue represented the abundance of different bacteria, the dark shade was high, and the light shade was low. Con, control; UC, ulcerative colitis.

and the abundance of *Deferribacteres* in the microflora, which was reduced by UC, was increased following treatment (38). Similarly, in the present study, the abundance of *Deferribacteres* in the UC + irisin group was higher compared with the UC group, and the symptoms of the UC model mice were alleviated by irisin treatment. Therefore, irisin may exert its anti-inflammatory effects by inducing alterations in the intestinal flora; however, the mechanism by which irisin affects intestinal microbiota needs further investigation.

Intestinal microbiota belong to a diverse anaerobic species and extraction may be challenging (39). Consequently, the mechanism underlying intestinal microbial alterations in UC is not completely understood. Previous studies have indicated that certain microorganisms produce a large number of metabolites that serve as a major source of intestinal antigens, resulting in an IgA-based antibody response (40,41). Frehn *et al* (42) observed a decrease in *E. coli*-specific antibody

IgA expression in the faeces of patients with UC. In the present study, high-throughput sequencing technology was used to analyse the composition and alterations to the intestinal flora in different groups more accurately and thoroughly compared with the detection of IgA antibody expression. Furthermore, quantitative comparisons were made at different taxonomic levels.

A number of studies have indicated that the occurrence of UC is not only related to intestinal microbiota alterations but is also related to alterations in the microbiota of the intestinal mucosal (27,43). The microbiota in the external and internal intestinal mucosal layers of patients with UC are significantly different compared with controls. Moreover, the compositional structure of the microbiota in the external mucosal layer, in which *Clostridium* is predominant, is significantly different compared with controls (44). Therefore, intestinal flora alterations may serve an important role during the progression of UC.

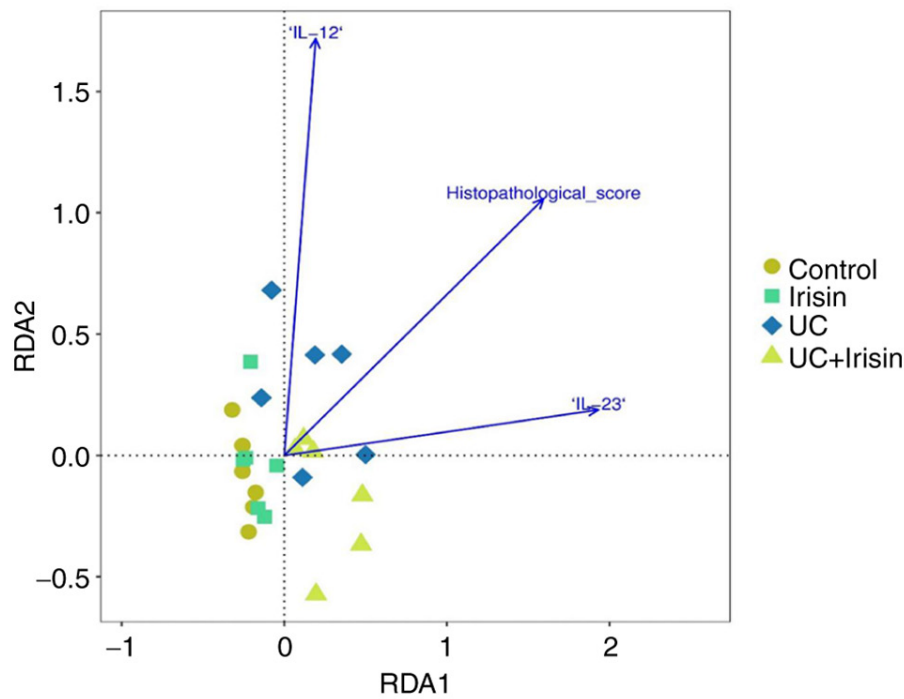


Figure 7. Association between the histopathological score and IL-12/23 levels. IL, interleukin; UC, ulcerative colitis; RDA, redundancy analysis.

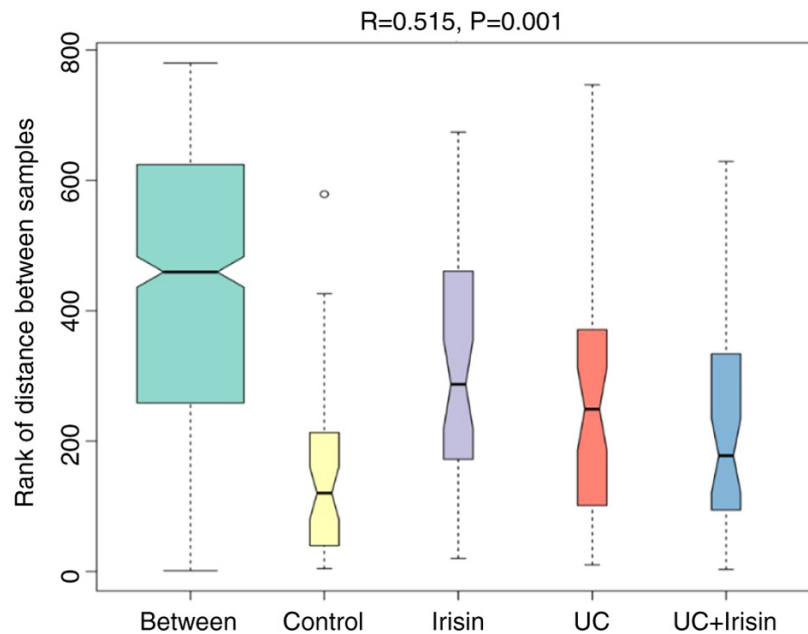


Figure 8. Differences in the microflora composition among the four groups. There was a significant difference among the four groups of samples. The circle in the control group represented an outlier. The R value was 0.515, and the P-value was 0.001, which indicates that the difference among the four groups of samples was significantly greater than those within the group. UC, ulcerative colitis.

Due to the differences in UC course, stages, treatments and analytical methods in each patient, as well as the complex structure and function of the intestinal flora, at present, there is no consensus regarding alterations in intestinal aerobic bacteria and common anaerobic bacteria in patients with UC. As a result, the specific roles of bacteria in the progression of the disease have not yet been fully elucidated, and alterations in the gut flora and their relationship with pathological changes in the intestinal mucosa remain unclear. To date, the

majority of studies have primarily focused on the relationship between a certain type of intestinal flora and UC; however, a comprehensive comparison between common intestinal flora and UC has not been performed. In the present study, a relatively thorough analysis of the intestinal microbiota in mice in each of the four groups was conducted.

To the best of our knowledge, a consensus regarding the anti-inflammatory mechanism underlying irisin has not been reached. Studies have indicated that irisin inhibits

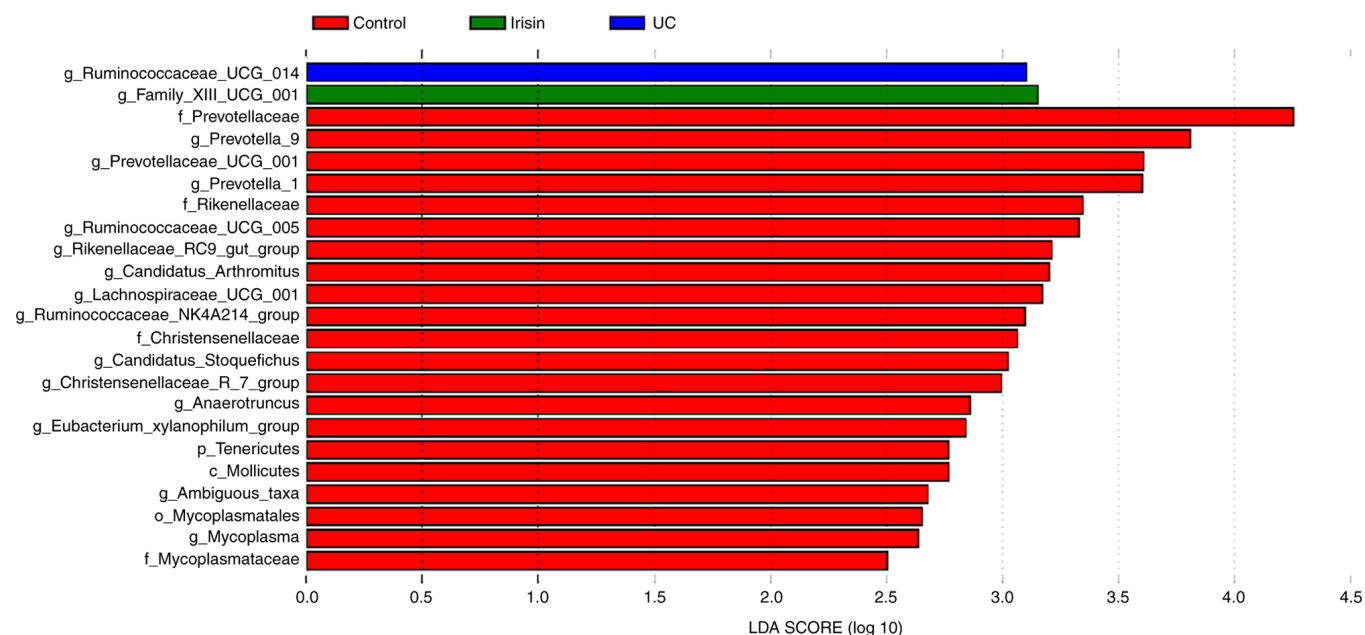


Figure 9. Microbiota that serve vital roles in each group. The UC + irisin group had no dominant bacteria. Con, control; UC, ulcerative colitis; LDA, linear discriminant analysis.

the inflammatory response and reduces pathological alterations during the progression of acute lung injury in a concentration-dependent manner (45,46). Irisin may reduce the expression of NF- $\kappa$ B (p65) in the nucleus and increase its expression level in the cytosol by inhibiting apoptosis (17). Mazur-Bialy *et al* (16) reported that lower concentrations of irisin can not only enhance the expression of TLR4 in macrophages, but can also promote the ability of macrophages to recognize potential pathogens, indirectly increasing anti-inflammatory effects. Furthermore, irisin also significantly reduces the levels of TLR4 and MyD88 protein in macrophages, as well as the phosphorylation of NF- $\kappa$ B, leading to a decreased release of key pro-inflammatory cytokines, which results in an anti-inflammatory effect. Another study also reported that the anti-inflammatory effect of irisin may be due an improvement in the levels of TNF- $\alpha$  and TNF superfamily member 11, two factors that drive lymph node hyperplasia (47). In the present study, the macroscopic and histopathological scores, the abundance of CD64<sup>+</sup> cells and the level of proinflammatory cytokines in the plasma, such as IL-12 and IL-23, were decreased in irisin-treated UC model mice compared with untreated UC model mice.

IL-12 is a heterodimer molecule composed of p40 and p35 subunits connected by disulfide bonds. Under physiological conditions, IL-12 is produced by mature dendritic cells and activated monocyte macrophages and provides important signals that promote the differentiation and proliferation of T helper (Th)1 cells, thereby participating in the inflammatory response (48). IL-23 is formed by p40 and p19 subunit chains and serves a key role in the differentiation and expansion of Th cells and resident lymphocytes (49,50). A previous study indicated that the expression level of IL-12 mRNA in UC is significantly increased compared with normal colon tissue and may serve an important role in the pathogenesis of UC (51). Another study reported that the p40 chain serves an important

role in intestinal inflammation (52). Genome-wide association studies have indicated that mutations in the gene encoding the IL-23 receptor and the site encoding the p40 gene are genetic risks for the development of UC (53,54). Monoclonal antibodies against the p40 chain blocked the activity of IL-12 and IL-23 and have displayed initial success for the treatment of UC (55). In the present study, the plasma levels of IL-12 and IL-23 in mice were significantly increased in UC model mice compared with control mice. The macroscopic score and histopathological score of UC model mice were significantly decreased by irisin treatment. Furthermore, the number of CD64<sup>+</sup> cells, and the plasma levels of IL-12 and IL-23 were also decreased in UC model mice following treatment with irisin.

During the present study, three mice died. The first death occurred in the UC group on day 5 of the experiment, and on day 6, two further deaths were recorded (one in the UC group and one in the UC + Irisin group). According to previous study (56), due to the mucosal damage and anticoagulation effects of DSS, the modest initial effects are followed by increasingly worsening symptoms, including increased intestinal permeability, severe bleeding and mortality. DSS-induced mortality can be variable dependent on the concentration and duration of treatment (57). Shimizu *et al* (58) reported that in a 4% DSS model, 2 out of 10 rats died before the day 7 of DSS administration, which was similar to the mortality rate of the present study. In addition, Axelsson *et al* (59) demonstrated that neither T, B nor NK cells were critical for the induction of DSS-induced colitis in mice. Administration of 5% DSS to athymic nu/nu CD-1(BR) mice resulted in a rapid decline in body weight and a short survival time, with no animals surviving beyond day 9. Furthermore, the administration of 5% DSS in SCID mice resulted in a 50% survival rate at day 9 of DSS administration. In order to minimize animal mortality in our preliminary experiments, an appropriate DSS load for the reliable induction of colitis and comparable severity



of disease between animals was established according to the method conducted by Vowinkel *et al* (60). The results of the preliminary experiments indicated that the protocol that was used in the present study led to lowest mortality rate, but still represented a classic UC model with obvious body weight loss and histological damage. The death of the three mice in the present study was caused by severe diarrhea, severe blood in the stool, dehydration, continuous weight loss and damage to the liver coagulation mechanism; however, the detailed mechanism underlying the death observed in the present study requires further investigation.

The present study demonstrated the anti-inflammatory effects of irisin, as well as the accompanied alterations to the intestinal microbiome. In addition, a possible preliminary relationship between the anti-inflammatory effect of irisin and alterations to the intestinal flora was identified. Future studies using specific order or gene knockout mice should be conducted to support the results of the present study. A limitation of the present study is that the relationship between alterations to the intestinal microbiota and inflammation is controversial. For example, colonic infusion of donor human intestinal flora can reverse UC in selected patients, which suggests that differences in the gut microbiota may be the cause of milder inflammation (61). However, by investigating the correlation between fecal flora alterations and inflammatory indicators, other studies have indicated that alterations to the gut microbiota may be a consequence of inflammation (62). Microbiota transferring artificial colonization with divergent species or other specific gnotobiotic techniques is a key strategy that could be used to explain the relationship between alterations to the intestinal microbiota and intestinal inflammation. Furthermore, only the anti-inflammatory effect of irisin was investigated in the present study; therefore, comparing irisin with other clinically used drugs requires further investigation.

In conclusion, the present study suggested that irisin ameliorated gut inflammation potentially by altering the gut microbiota in UC model mice. Therefore, irisin may serve as a novel therapeutic agent for UC.

## Acknowledgements

Not applicable.

## Funding

The present study was supported by the National Natural Science Foundation of China (grant nos. 81500430 and U1304802 to XHL), the Key Project of Science and Technology Research of the Education Department of Henan (grant nos. 17A320019 to HCW), the Henan Science and Technology Planning Project (grant nos. 182102310544 and 192102310045 to XHL; grant no. 182102310566 to HCW; grant no. 182102310567 to RLY) and the Henan Medical Science and Technology Tackling Project (grant no. 201702136 to ZFD).

## Availability of data and materials

The datasets used and analyzed during the current study are available from the corresponding author on reasonable request.

## Authors' contributions

LXH and XTC performed the histopathological examination and immunofluorescence experiment, and contributed equally to this paper. XHL designed the research study. RLY conducted IL-12 and IL-18 measurement, and the correlation analysis. RLY and LXH confirmed the authenticity of the raw data. JNY and HCW helped to interpret and analyze the data. ZFD and YXL conducted high throughput sequencing experiments. XTC and XHL revised the work critically for important intellectual content. All authors read and approved the final manuscript.

## Ethics approval and consent to participate

The animal experiments were approved by the Medical Ethics Committee of Henan University (approval no. HUSOM2020-103).

## Patient consent for publication

Not applicable.

## Competing interests

The authors declare that they have no competing interests.

## References

1. Anzai H, Hata K, Kishikawa J, Ishii H, Yasuda K, Otani K, Nishikawa T, Tanaka T, Kiyomatsu T, Kawai K, *et al*: Appendiceal orifice inflammation is associated with proximal extension of disease in patients with ulcerative colitis. *Colorectal Dis* 18: 0278-0282, 2016.
2. Podolsky DK: Inflammatory bowel disease. *N Engl J Med* 347: 417-429, 2002.
3. Grinspan A and Kornbluth A: Positioning therapy for ulcerative colitis. *Curr Gastroenterol* 17: 29, 2015.
4. Khor B, Gardet A and Xavier RJ: Genetics and pathogenesis of inflammatory bowel disease. *Nature* 474: 307-317, 2011.
5. Legaki E and Gazouli M: Influence of environmental factors in the development of inflammatory bowel diseases. *World J Gastrointest Pharmacol Ther* 7: 112-125, 2016.
6. Frank DN, St Amand AL, Feldman RA, Boedeker EC, Harpaz N and Pace NR: Molecular-phylogenetic characterization of microbial community imbalances in human inflammatory bowel diseases. *Proc Natl Acad Sci USA* 104: 13780-13785, 2007.
7. Ihara S, Hirata Y and Koike K: TGF- $\beta$  in inflammatory bowel disease: A key regulator of immune cells, epithelium, and the intestinal microbiota. *J Gastroenterol* 52: 777-787, 2017.
8. Manichanh C, Rigottier-Gois L, Bonnaud E, Gloux K, Pelletier E, Frangeul L, Nalin R, Jarrin C, Chardon P, Marteau P, *et al*: Reduced diversity of faecal microbiota in Crohn's disease revealed by a metagenomic approach. *Gut* 55: 205-211, 2006.
9. Schwab C, Berry D, Rauch I, Rennisch I, Ramesmayer J, Hainzl E, Heider S, Decker T, Kenner L, Muller M, *et al*: Longitudinal study of murine microbiota activity and interactions with the host during acute inflammation and recovery. *ISME J* 8: 1101-1114, 2014.
10. Boström P, Wu J, Jedrychowski MP, Korde A, Ye L, Lo JC, Rasbach KA, Boström EA, Choi JH, Long JZ, *et al*: A PGC1- $\alpha$ -dependent myokine that drives brown-fat-like development of white fat and thermogenesis. *Nature* 481: 463-468, 2012.
11. Yi Z, Yi S and Shu-Zhe D: The novel Myokine-Irisin. *Chin J Biochem Mol Biol* 33: 429-435, 2017.
12. Farmer SR: Boning up on Irisin. *N Engl J Med* 380: 1480-1482, 2019.
13. Mahgoub MO, D'Souza C, Al Darmaki RSMH, Baniyas MMYH and Adeghate E: An update on the role of irisin in the regulation of endocrine and metabolic functions. *Peptides* 104: 15-23, 2018.

14. Buscemi S, Corleo D, Vasto S, Buscemi C, Barile AM, Rosafio G, Randazzo C, Currenti W and Galvano F: Serum Irisin concentrations in severely inflamed patients. *Horm Metab Res* 52: 246-250, 2020.
15. Mazur-Bialy AI: Superiority of the Non-glycosylated form over the glycosylated form of Irisin in the attenuation of adipocytic meta-inflammation: A potential factor in the fight against insulin resistance. *Biomolecules* 9: 394, 2019.
16. Mazur-Bialy AI, Pocheć E and Zarawski M: Anti-inflammatory properties of Irisin, mediator of physical activity, are connected with TLR4/MyD88 signaling pathway activation. *Int J Mol Sci* 18: 701-712, 2017.
17. Shao L, Meng D, Yang F, Haibo S and Dongqi T: Irisin-mediated protective effect on LPS-induced acute lung injury via suppressing inflammation and apoptosis of alveolar epithelial cells. *Biochem Biophys Res Commun* 487: 194-200, 2017.
18. Mazur-Bialy AI, Bilski J, Wojcik D, Brzozowski B, Surmiak M, Hubalewska-Mazgaj M, Chmura A, Magierowski M, Magierowska K, Mach T and Brzozowski T: Beneficial effect of voluntary exercise on experimental colitis in mice fed a High-Fat Diet: The role of Irisin, adiponectin and proinflammatory biomarkers. *Nutrients* 9: 410, 2017.
19. Asadi Y, Gorjipour F, Behrouzifar S and Vakili A: Irisin peptide protects brain against ischemic injury through reducing apoptosis and enhancing BDNF in a rodent model of stroke. *Neurochem Res* 43: 1549-1560, 2018.
20. Pitts M and Applied Research Ethics National Association/Office of Laboratory Animal Welfare. Institutional Animal Care and Use Committee: A Guide to the New ARENA/OLAW IACUC Guidebook. *Lab Anim (NY)* 31: 40-42, 2002.
21. Siegmund B, Lehr HA, Fantuzzi G and Dinarello CA: IL-1 $\beta$ -converting enzyme (caspase-1) in intestinal inflammation. *Proc Natl Acad Sci USA* 98: 13249-13254, 2001.
22. Murano M, Maemura K, Hirata I, Toshina K, Nishikawa T, Hamamoto N, Sasaki S, Saitoh O and Katsu K: Therapeutic effect of intracolonic administered nuclear factor kappa B (p65) antisense oligonucleotide on mouse dextran sulphate sodium (DSS)-induced colitis. *Clin Exp Immunol* 120: 51-58, 2000.
23. Jumpstart Consortium Human Microbiome Project Data Generation Working Group: Evaluation of 16S rDNA-based community profiling for human microbiome research. *PLoS One* 7: e39315, 2012.
24. Ng SC, Shi HY, Hamidi N, Underwood FE, Tang W, Benchimol EI, Panaccione R, Ghosh S, Wu JCY, Chan FKL, *et al*: Worldwide incidence and prevalence of inflammatory bowel disease in the 21st century: A systematic review of population-based studies. *Lancet* 390: 2769-2778, 2018.
25. Porter RJ, Kalla R and Ho GT: Ulcerative colitis: Recent advances in the understanding of disease pathogenesis. *F1000Res* 9: F1000, 2020.
26. Colquhoun C, Duncan M and Grant G: Inflammatory bowel diseases: Host-microbial-environmental interactions in dysbiosis. *Diseases* 8: E13, 2020.
27. Kaser A, Zeissig S and Blumberg RS: Inflammatory bowel disease. *Annu Rev Immunol* 28: 573-621, 2010.
28. Martini E, Krug SM, Siegmund B, Neurath MF and Becker C: Mend your fences: The epithelial barrier and its relationship with mucosal immunity in inflammatory bowel disease. *Cell Mol Gastroenterol Hepatol* 4: 33-46, 2017.
29. Qin J, Li R, Raes J, Arumugam M, Burgdorf KS, Manichanh C, Nielsen T, Pons N, Levenez F, Yamada T, *et al*: A human gut microbial gene catalogue established by metagenomic sequencing. *Nature* 464: 59-65, 2010.
30. Etienne-Mesmin L, Chassaing B, Desvaux M, De Paepe K, Gresse R, Sauvatre T, Forano E, de Wiele TV, Schüller S, Juge N and Blanquet-Diot S: Experimental models to study intestinal microbes-mucus interactions in health and disease. *FEMS Microbiol Rev* 43: 457-489, 2019.
31. O'Callaghan AA and Corr SC: Establishing boundaries: The relationship that exists between intestinal epithelial cells and gut-dwelling bacteria. *Microorganisms* 7: Efficiency of cancer therapy. *Front Microbiol* 10: 1050, 2019.
32. Ma W, Mao Q, Xia W, Dong G, Yu C and Jiang F: Gut microbiota shapes the efficiency of cancer therapy. *Front Microbiol* 10: 1050, 2019.
33. Mika A, Van Treuren W, González A, Herrera JJ, Knight R and Fleshner M: Exercise is more effective at altering gut microbial composition and producing stable changes in lean mass in juvenile versus adult male F344 rats. *PLoS One* 10: e0125889, 2015.
34. Mohr AE, Jäger R, Carpenter KC, Kerkick CM, Purpura M, Townsend JR, West NP, Black K, Gleeson M, Pyne DB, *et al*: The athletic gut microbiota. *J Int Soc Sports Nutr* 17: 24, 2020.
35. Luo B, Xiang D, Nieman DC and Chen P: The effects of moderate exercise on chronic stress-induced intestinal barrier dysfunction and antimicrobial defense. *Brain Behav Immunity* 39: 99-106, 2014.
36. Clarke SF, Murphy EF, O'Sullivan O, Lucey AJ, Humphreys M, Hogan A, Hayes P, O'Reilly M, Jeffery IB, Wood-Martin R, *et al*: Exercise and associated dietary extremes impact on gut microbial diversity. *Gut* 63: 1913-1920, 2014.
37. Allen JM, Berg Miller ME, Pence BD, Whitlock K, Nehra V, Gaskins HR, White BA, Fryer JD and Woods JA: Voluntary and forced exercise differentially alters the gut microbiome in C57BL/6J mice. *J Appl Physiol* 118: 1059-1066, 2015.
38. Yang Y, Gang C, Qian Y, Juan Y, Xueting C, Pamo T, Xiaolan C, Chunping H, Shuangquan Z and Peng C: Gut microbiota drives the attenuation of dextran sulphate sodium-induced colitis by Huangqin decoction. *Oncotarget* 8: 48863-48874, 2017.
39. Liu JH, Chen ZL, Li Y and Yu DJ: Development of denaturing gradient gel electrophoresis for analysis of intestinal microflora community diversity. *Chin J Veterinary Sci Technol* 35, 2006.
40. Donaldson GP, Ladinsky MS, Yu KB, Sanders JG, Yoo BB, Chou WC, Conner ME, Earl AM, Knight R, Bjorkman PJ and Mazmanian SK: Gut microbiota utilize immunoglobulin A for mucosal colonization. *Science* 360: 795-800, 2018.
41. Moor K, Diard M, Sellin ME, Felmy B, Wotzka SY, Toska A, Bakkeren E, Arnoldini M, Bansept F, Co AD, *et al*: High-avidity IgA protects the intestine by enchainning growing bacteria. *Nature* 544: 498-502, 2017.
42. Frehn L, Jansen A, Bennek E, Mandic AD, Temizel I, Tischendorf S, Verdier J, Tacke F, Streetz K, Trautwein C and Sellge G: Distinct patterns of IgG and IgA against food and microbial antigens in serum and feces of patients with inflammatory bowel diseases. *PLoS One* 9: e106750, 2014.
43. Kurashima Y and Kiyono H: Mucosal ecological network of epithelium and immune cells for gut homeostasis and tissue healing. *Annu Rev Immunol* 35: 119-147, 2017.
44. Pei LY, Ke YS, Zhao HH, Wang L, Jia C, Liu WZ, Fu QH, Shi MN, Cui J and Li SC: Role of colonic microbiota in the pathogenesis of ulcerative colitis. *BMC Gastroenterol* 19: 10, 2019.
45. Li X, Jamal M, Guo P, Jin Z, Zheng F, Song X, Zhan J and Wu H: Irisin alleviates pulmonary epithelial barrier dysfunction in sepsis-induced acute lung injury via activation of AMPK/SIRT1 pathways. *Biomed Pharmacother* 118: 109363, 2019.
46. Chen K, Xu Z, Liu Y, Wang Z, Li Y, Xu X, Chen C, Xia T, Liao Q, Yao Y, *et al*: Irisin protects mitochondria function during pulmonary ischemia/reperfusion injury. *Sci Transl Med* 9: ea06298, 2017.
47. Narayanan SA, Metzger CE, Bloomfield SA and Zawieja DC: Inflammation-induced lymphatic architecture and bone turnover changes are ameliorated by Irisin treatment in chronic inflammatory bowel disease. *FASEB J* 32: 4848-4861, 2018.
48. Murphy KM, Ouyang W and Farrar JD: Signaling and transcription in T helper development. *Annu Rev Immunol* 18: 451-494, 2000.
49. Fuss JJ, Becker C, Yang Z, Groden C, Hornung RL and Heller F: Both IL-12p70 and IL-23 are synthesized during active Crohn's disease and are down-regulated by treatment with anti-IL-12 p40 monoclonal antibody. *Inflamm Bowel Dis* 12: 9-15, 2006.
50. Grivennikov DI, Wang K, Mucida D, Wewurtel C, Schnabl B and Jauch D: Adenoma-linked barrier defects and microbial products drive IL-23/IL-17-mediated tumor growth. *Nature* 491: 254-258, 2012.
51. Wang BY, Liu FL, Hu Z, Yu CH, Xia XT, Fan JY and Li X: Effects of Tongxieyaofang on serum levels of interleukin-12 and neuropeptide Y in rats with ulcerative colitis. *Hun J Traditional Chin Med* 32: 166-167, 2016.
52. Fiorino G, Allocca M, Correale C, Roda G, Furfaro F, Loy L, Zilli A, Peyrin-Biroulet L and Danese S: Positioning ustekinumab in moderate-to-severe ulcerative colitis: New kid on the block. *Expert Opin Biol Ther* 20: 421-427, 2020.
53. Beaudoin M, Goyette P, Boucher G, Lo KS, Rivas MA, Stevens C, Alikashani A, Ladouceur M, Ellinghaus D, Törkvist L, *et al*: Deep resequencing of GWAS loci identifies rare variants in CARD9, IL23R and RNFI86 that are associated with ulcerative colitis. *PLoS Genet* 9: e1003723, 2013.
54. Bianchi E and Rogge L: The IL-23/IL-17 pathway in human chronic inflammatory diseases-new insight from genetics and targeted therapies. *Microbes Infect* 21: 246-253, 2019.

55. Niederreiter L, Adolph TE and Kaser A: Anti-IL-12/23 in Crohn's disease: Bench and bedside. *Curr Drug Targets* 14: 1379-1384, 2013.
56. Eichele DD and Kharbanda KK: Dextran sodium sulfate colitis murine model: An indispensable tool for advancing our understanding of inflammatory bowel diseases pathogenesis. *World J Gastroenterol* 23: 6016-6029, 2017.
57. Chassaing B, Aitken JD, Malleshappa M and Vijay-Kumar M: Dextran sulfate sodium (DSS)-induced colitis in mice. *Curr Protoc Immunol* 104: 15.25.1-15.25.14, 2014.
58. Shimizu T, Suzuki M, Fujimura J, Hisada K, Yoshikazu O, Obinata K and Yamashiro Y: The relationship between the concentration of dextran sodium sulfate and the degree of induced experimental colitis in weanling rats. *Pediatr Gastroenterol Nutr* 37: 481-486, 2003.
59. Axelsson LG, Landström E, Goldschmidt TJ, Grönberg A and Bylund-Fellenius AC: Dextran sulfate sodium (DSS) induced experimental colitis in immunodeficient mice: Effects in CD4(+) -cell depleted, athymic and NK-cell depleted SCID mice. *Inflamm Res* 45: 181-191, 1996.
60. Vowinkel T, Kalogeris TJ, Mori M, Krieglstein CF and Granger DN: Impact of dextran sulfate sodium load on the severity of inflammation in experimental colitis. *Dig Dis Sci* 49: 556-564, 2004.
61. Borody TJ, Warren EF, Leis S, Surace R and Ashman O: Treatment of ulcerative colitis using fecal bacteriotherapy. *Clin Gastroenterol* 37: 42-47, 2003.
62. Zhang T, Chen Y, Wang Z, Zhou Y, Zhang S, Wang P, Xie S and Jiang B: Changes of fecal flora and its correlation with inflammatory indicators in patients with inflammatory bowel disease. *Nan Fang Yi Ke Da Xue Xue Bao* 33: 1474-1477, 2013 (In Chinese).



This work is licensed under a Creative Commons Attribution-NonCommercial-NoDerivatives 4.0 International (CC BY-NC-ND 4.0) License.